Journal of Applied Polymer Science

Micromechanical Analysis of Long Fiber-Reinforced Composites with Nanoparticle Incorporation into the Interphase Region

Xiaoqiang Wang, Weitao Zhao, Bo Fang, Shaowei Lu, Yewei Zhang
Faculty of Aerospace Engineering, Shenyang Aerospace University, Shenyang 110136, China
Correspondence to: X. Wang (E-mail: xqwang_sau@163.com)

ABSTRACT: The influence of the distribution type, Young's modulus, and volume fraction of the nanoparticles within the interphase region on the mechanical behavior of long fiber-reinforced composites with epoxy resin matrix under transverse tensile loading is investigated in this article. An infinite material containing unidirectional long fiber and periodic distribution of elastic, spherical nanoparticles was modeled using a unit cell approach. A stiffness degradation technique has been used to simulate the damage and crack progress of the matrix subjected to mechanical loading. A series of computational experiments performed to study the influence of the nanoparticle indicate that the mechanical properties, nanoparticle-fiber distance, and volume fraction of nanoparticle have a significant effect on both the stiffness and strength properties of these composite materials. © 2014 Wiley Periodicals, Inc. J. Appl. Polym. Sci. **2015**, *132*, 41573.

KEYWORDS: composites; microscopy; nanoparticles; nanowires and nanocrystals; nanostructured polymers; theory and modeling

Received 8 April 2014; accepted 25 September 2014
DOI: 10.1002/app.41573

INTRODUCTION

Long fiber-reinforced composites (LFRCs) used in lightweight structures have been found numerous applications in aerospace industry for their high specific strength and stiffness.[1] The increasing use of these materials in the industries requires efficient technologies to predict the mechanical behaviors of such composites. The current trend of work to address the industry's requirement is to complement it with new micromechanical numerical method.[2] Computational micromechanics,[3] also defined as virtual test and virtual experiment in different literature, are widely applied to analyze the influence of the microstructure and phase properties of composites on their stiffness and strength properties. Compared to the actual experiments, the virtual test presents three important advantages from a mechanical point of view. First, we can easily apply multiaxial loading condition to the composite materials. Second, we can study the influence of the reinforcement (distribution of shape, spatial, size, etc.), interphase and matrix on the macroscale response of composites. Third, we can access the detailed microscale stress–strain fields and failure evolution during the loading process.

A number of micromechanical methodologies are developed to predict the composite mechanical properties. Shan and Gokhale[4] developed a sufficiently small microstructural window that can be regarded as a representative volume element (RVE) of a nonuniform microstructure of a ceramic matrix composite containing a range of fiber sizes, and fiber-rich and -poor regions at the length scale of about 100 μm. A three-dimensional (3D) finite-element micromechanical model was developed to study interface damage of metal matrix composites subjected to transverse loading by Aghdam and Falahatgar.[5] By means of the generalized method of cells as the micromechanical model, the overall effective properties of the composite were quantified by Matzenmiller and Gerlach.[6] A program is developed to generate two-dimensional (2D) micromechanical FE-model for Metal matrix composite by Hai Qing.[7] And a series of computational experiments are performed to study the influence of particle arrangements, interface strengths and loading conditions of the RVE on composite stiffness and strength properties. Shokrieh calculated the longitudinal strength of unidirectional E-glass/epoxy composites exposed to sulfuric acid environment using the micromechanics theorem.[8] A 3D microstructures of syntactic foams with different degrees of particle clustering were reconstructed based on random sequential adsorption method by Ming Yu, and the progressive damage behavior were investigated.[9] The effect of the randomness of fiber distribution on the transverse modulus is investigated by using ABAQUS micromechanical analysis by Wang.[10] Sozhamannan discussed the methodology of microstructure based elastic-plastic finite-element analysis of particle reinforced metal matrix composites.[11]

The combination of various modifications on different hierarchically levels can ideally lead to an increased overall performance of LFRCs. It is well known, that LFRCs failure is often

© 2014 Wiley Periodicals, Inc.

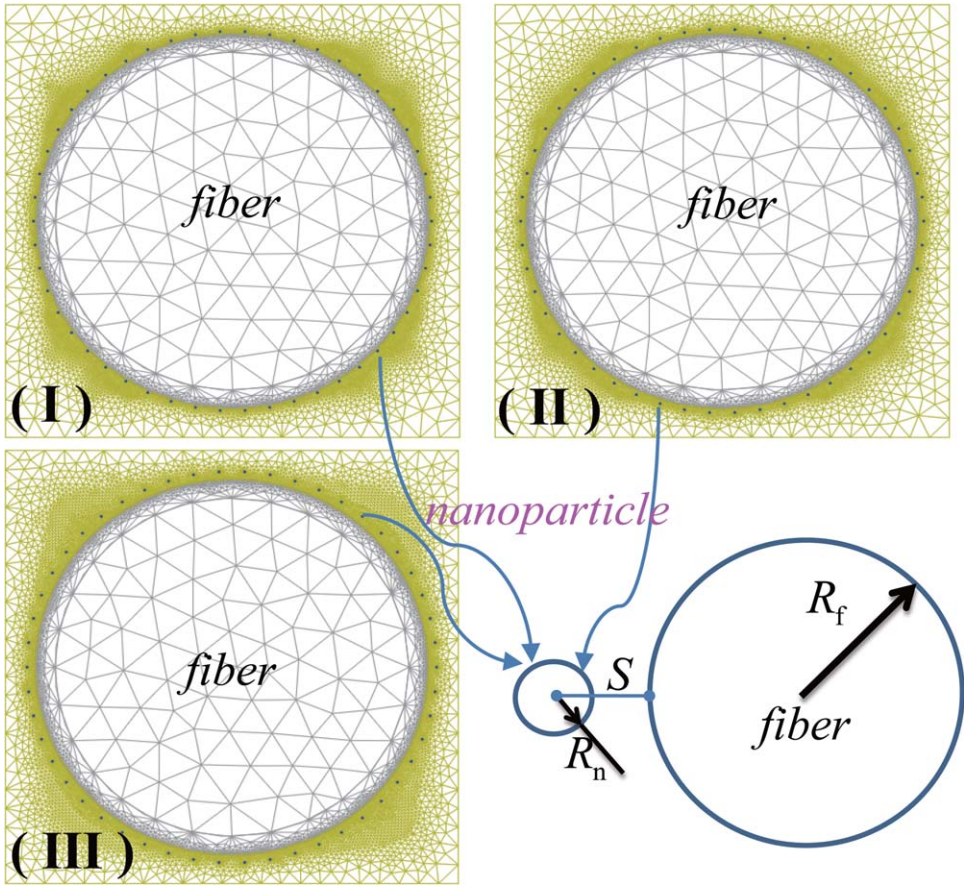

Figure 1. Models with different nanoparticle-fiber space distance *S*. [Color figure can be viewed in the online issue, which is available at wileyonlinelibrary.com.]

determined by matrix behavior caused by indifferent loading conditions. Studies have shown that nanoscaled particles can improve the matrix properties and are currently the subject of international research that show remarkable improvements in mechanical and thermal characteristics compared with pure resins.[12–15] Tjong has reviewed the state-of-the-art processing methods, structures and mechanical properties of the metal matrix composites reinforced with ceramic nanoparticles.[16] Vassileva and Friedrich studied the influence of alumina nanoparticle addition on the dynamic mechanical spectra of an amino-cured epoxy resin.[17] Maija developed an effective method for dispersing SiO_2 nanoparticles into polyethylene and the effects of nanoparticle on the mechanical properties of nanocomposites have been evaluated.[18] Amitava reported the development and characterization of carbon nanofiber-incorporated carbon/phenolic multiscale composites.[19] The work in this paper was inspired by the idea that nanoscaled particles could lead to a strengthened matrix as well as a stronger fiber/matrix interphase. With thus strengthened fiber/matrix interphase LFRC materials with considerably improved mechanical properties are accessible.[20,21] Furthermore, both fiber-reinforced composites and particle-reinforced composites are involved in all the previous researches. In view of that, micromechanical analysis allows for a detailed insight of the mechanical behavior of a composite by considering the influence of each constituent. And the properties of interphases region can significantly affect the overall mechanical properties of the fiber- and particle-reinforced composites. The aim of this study was to develop a new micromechanical methodology which can be used to better understand the fracture mechanism of epoxy-based nanocomposites reinforced by both long fiber and nanoparticle. In this article, a 2D micromechanical unit cell model of fiber-reinforced composites with nanoparticles was generated by using finite-element software ABAQUS. The model was used to predict the mechanical behavior of nanoparticle-fiber-reinforced composites which contain one layer or multilayer of nanoparticles in the interphase region. A series of computational experiments were performed to estimate the effects of nanoparticle-fiber space distance and number of nanoparticle/layer. Meanwhile, the influence of nanoparticle Young's modulus on composite stiffness and strength properties was evaluated.

GENERATION OF 2D MICROMECHANICAL UNIT CELL MODEL OF FIBER-REINFORCED COMPOSITES WITH NANOPARTICLE

The Generation of Finite-Element Unit Cell Model

Composite materials properties, for example, strength and stiffness, are dependent on the volume fraction of the reinforced materials and individual properties of the constituent materials and the estimation of damage and failure progression is complex if compared to that of conventional metallic materials. In the micromechanical analysis, the constituent materials and

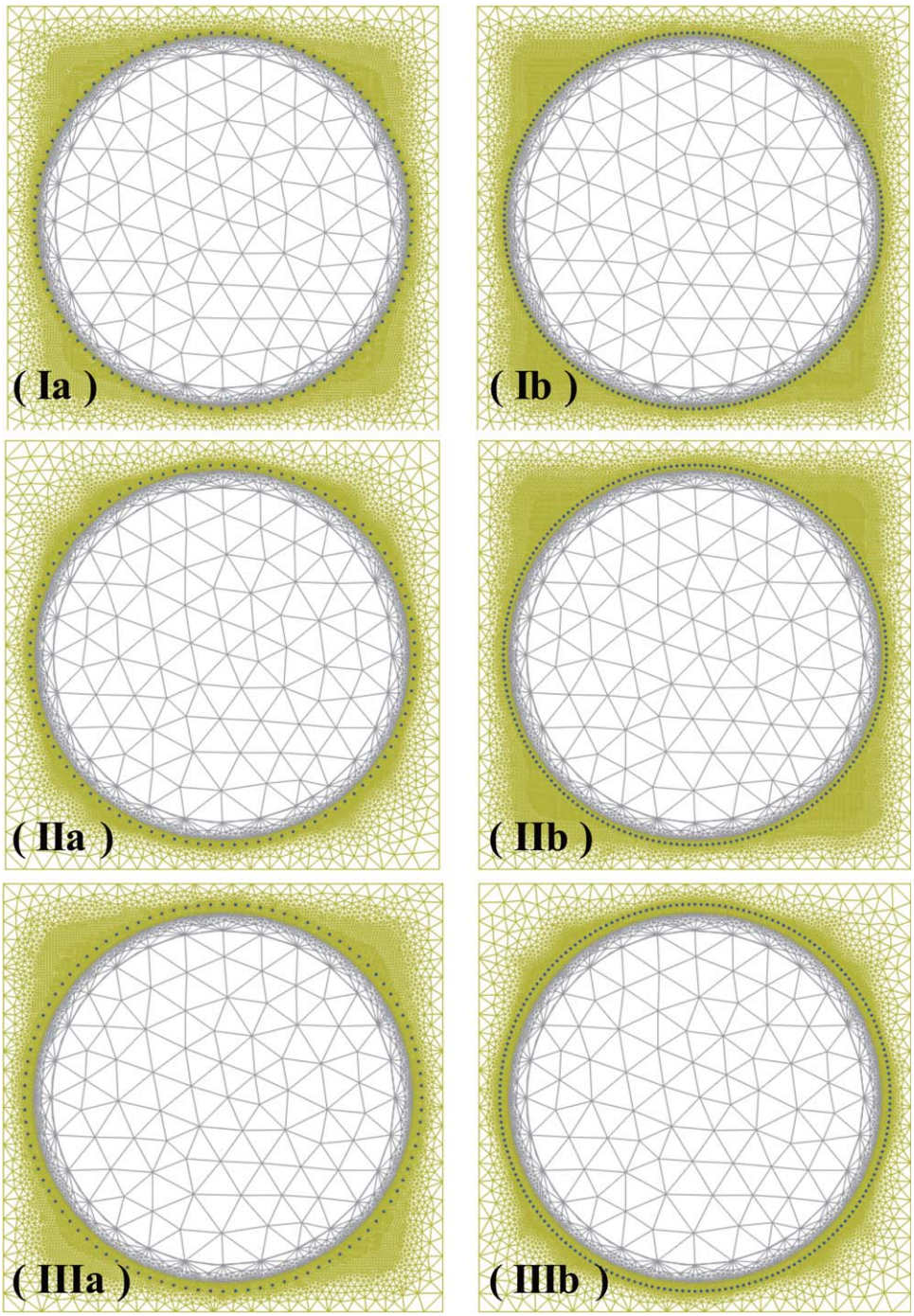

Figure 2. Models contain only one layer of nanoparticle with different nanoparticle numbers. [Color figure can be viewed in the online issue, which is available at wileyonlinelibrary.com.]

their interaction are distinctively considered to predict the overall mechanical behavior of the composite materials. The advantage of the micromechanical model is that the stresses can be associated and related to each constituent material. Therefore, failure can be identified in each of these constituents and the appropriate property degradation can be modeled.

Here, in order to study the influence of the nanoparticle-fiber space distance on damage behavior in LFRCs, three models with different nanoparticle-fiber space distance are built as shown in Figure 1. For the interphase region, which exists between the fiber and matrix, has a thickness of about 100 nm.[22] The space distance *S* between nanoparticle and fiber is set to be 40, 100, and 200 nm in model I, model II, and model III, respectively in the study. For simplicity and in order to compare the effect of nanoparticle distribution, 40, 100, and 200 nm are chosen. About 40 nm represents that the nanoparticles are within the interphase region. About 200 nm represents that the nanoarticles are without the interphase region. While 100 nm represents that the nanoparticles are on

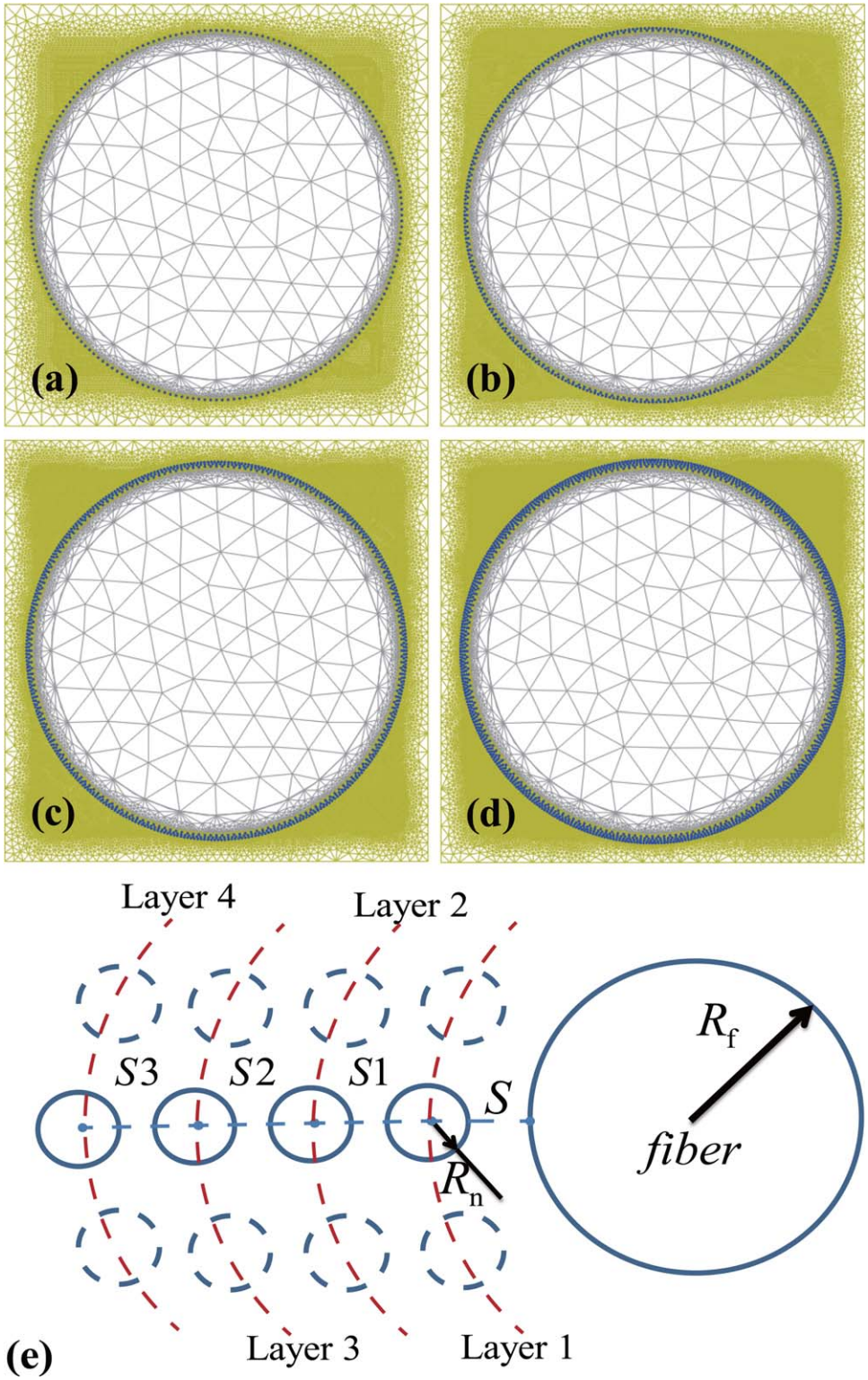

Figure 3. (a–d) Models contain one layer, two layers, three layers, and four layers of nanoparticle; (e) the arrangement order of nanoparticle layer around the fiber. [Color figure can be viewed in the online issue, which is available at wileyonlinelibrary.com.]

the interphase boundary. The radius R_n of all the nanoparticles is set to be 20 nm. The radius R_f of the fiber is set to be 5 μm. Each unit cell model has only one fiber and 50 nanoparticles with uniform distribution around the fiber. The volume fraction of fiber is 50%.

In order to study the influence of nanoparticle number on the damage behavior in LFRCs, several models which contain only one layer of nanoparticle with different nanoparticle numbers are built as shown in Figure 2. The space distance S between nanoparticle and fiber is 40, 100, and 200 nm in model Ia-b,

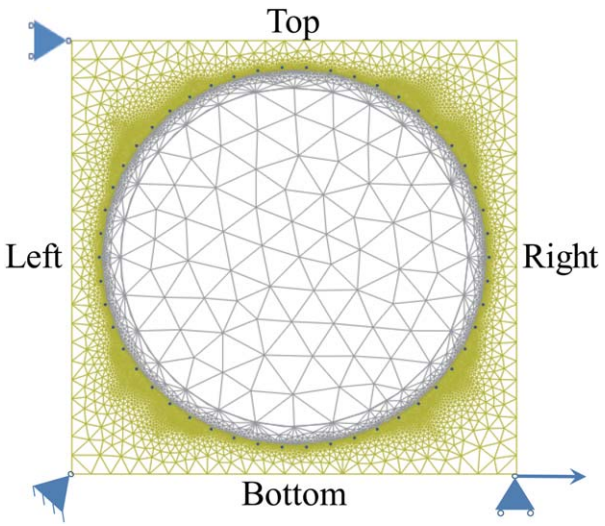

Figure 4. Periodic boundary conditions applied to unit cell model. [Color figure can be viewed in the online issue, which is available at wileyonlinelibrary.com.]

IIa-b, and IIIa-b, respectively. And, model Ia, IIa, and IIIa contain 100 nanoparticles while model Ib, IIb, and IIIb contain 200 nanoparticles around the fiber, respectively.

In order to investigate the effect of nanoparticle on the mechanical properties in long fiber composites with multi-layer nanoparticles, four models contain one layer, two layers, three layers, and four layers of nanoparticle are built as shown in Figure 3(a–d), respectively. Figure 3e shows the order of nanoparticle layer around the fiber. The space distance S between first layer of nanoparticle and fiber is 40 nm. The internanoparticle layer space is $S1=S2=S3=60$nm. The distribution of each layer of nanoparticle is uniform around the center fiber. Moreover, first layer, second layer, third layer, and fourth layer contain 200, 300, 350, and 400 nanoparticles, respectively.

Periodic boundary conditions are applied to the unit cells as shown in Figure 4. The periodic boundary conditions can be expressed as follows[23]:

$$\mathbf{u}_R-\mathbf{u}_{RB}=\mathbf{u}_L-\mathbf{u}_{LB} \quad (1)$$

$$\mathbf{u}_T-\mathbf{u}_{LT}=\mathbf{u}_B-\mathbf{u}_{LB} \quad (2)$$

where $\mathbf{u}$ is the displacement vector of any node on the boundary, and subscripts L, R, B, and T refer to the left, right, bottom and top edges, while subscripts with two letters correspond to the vertexes of the unit cell. The left-bottom vertex is constrained to prevent rigid body motions and the displacements of the left-top and right-bottom vertexes are suppressed in the horizontal and vertical directions, respectively, and then horizontal displacement (positive for tension and negative for compression) is applied incrementally to the right-bottom vertex until final fracture happens.

As fiber fracture and nanoparticle fracture is unlikely to happen under transverse loading, no damage model has been implemented for them, which are modeled as linear elastic and isotropic solids with the Young's modulus $E_f=77$ GPa, $E_n=10$ GPa, and Poisson's ratio $\upsilon_f=0.2$, $\upsilon_n=0.17$, respectively (Subscripts f and n are for fiber and nanoparticle, respectively).[24–26] FEM models are generated in ABAQUS/Standard. The whole model was meshed with 3-node triangle elements (CPE3). Free mesh technique was used for meshing, and mapped meshing

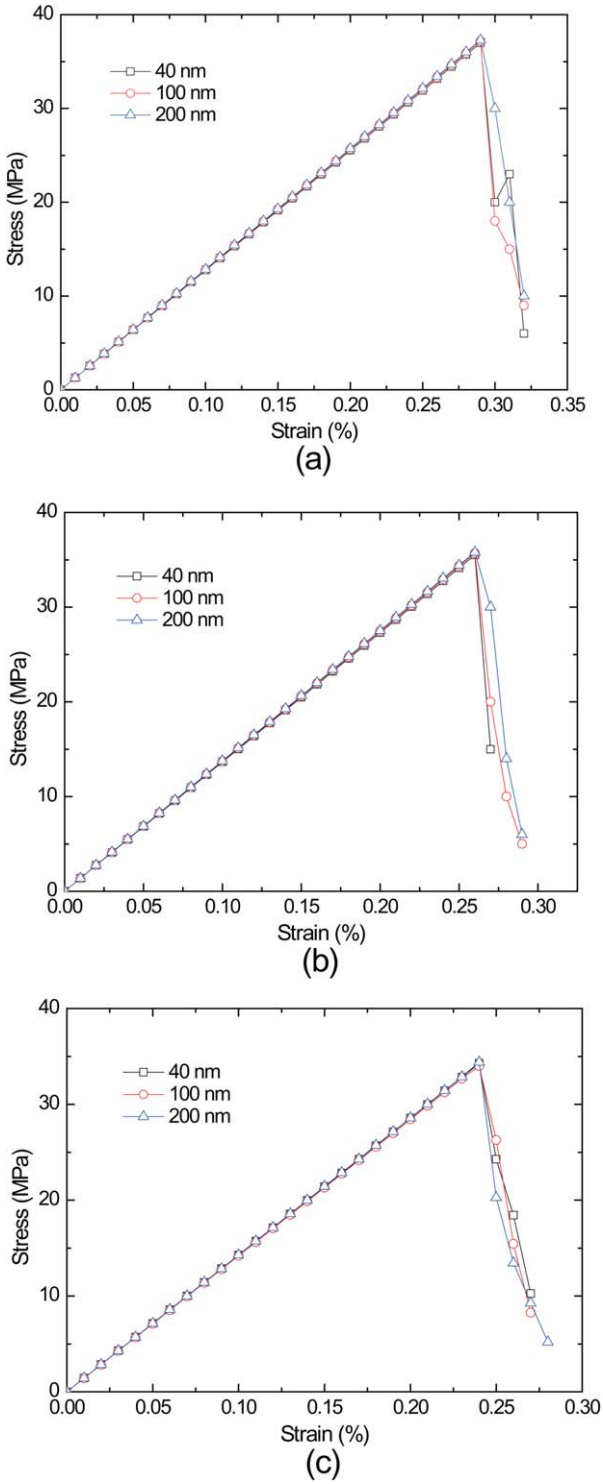

Figure 5. Stress–strain relationships when the nanoparticle number is 50, 100, and 200, respectively. [Color figure can be viewed in the online issue, which is available at wileyonlinelibrary.com.]

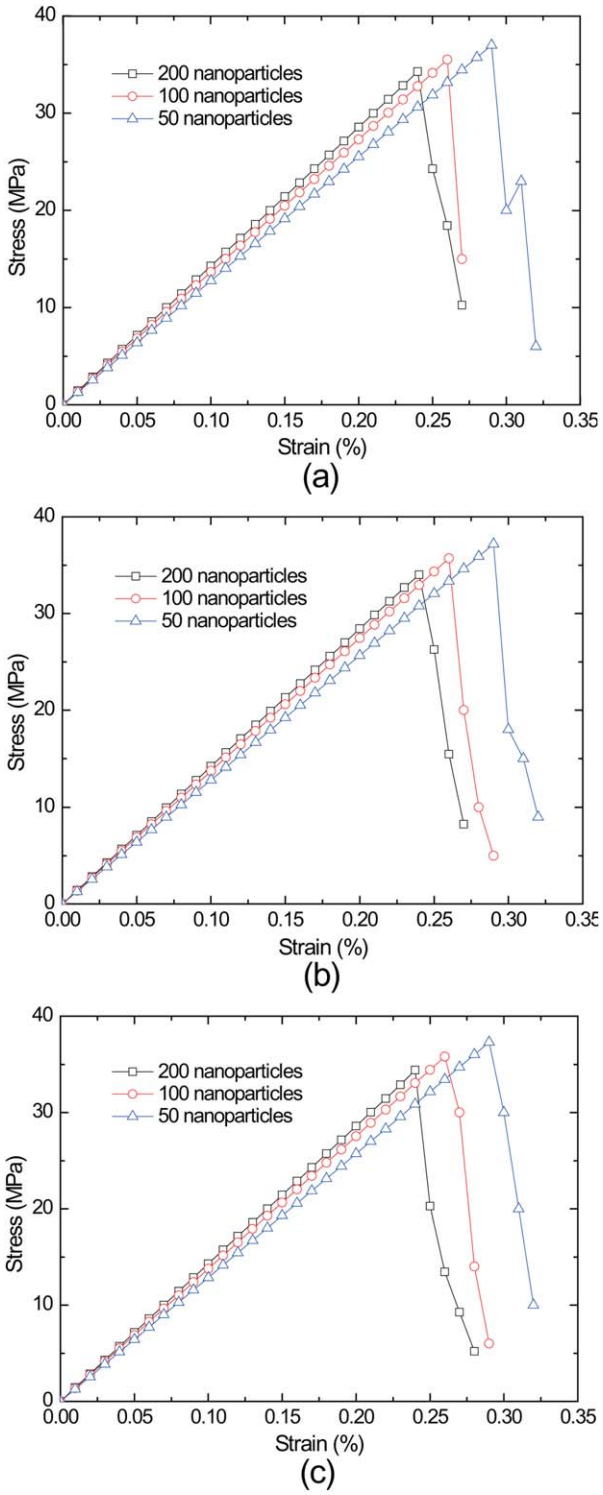

Figure 6. Stress–strain relationships when the nanoparticle-fiber space distance is 40, 100, and 200 nm, respectively. [Color figure can be viewed in the online issue, which is available at wileyonlinelibrary.com.]

algorithm was used where appropriate. The models contain approximately 25,000 (one layer of nanoparticle) to 65,000 (four layers of nanoparticle) elements. Intel Core i3-3110M CPU was used for the simulations.

Damage Mechanism and Mechanical Properties of Polymeric Matrix

In polymeric matrix, the yield behavior is sensitive to hydrostatic stress and as a consequence, the yield stress in tension is different from that in compression.[27,28] Based on a local damage

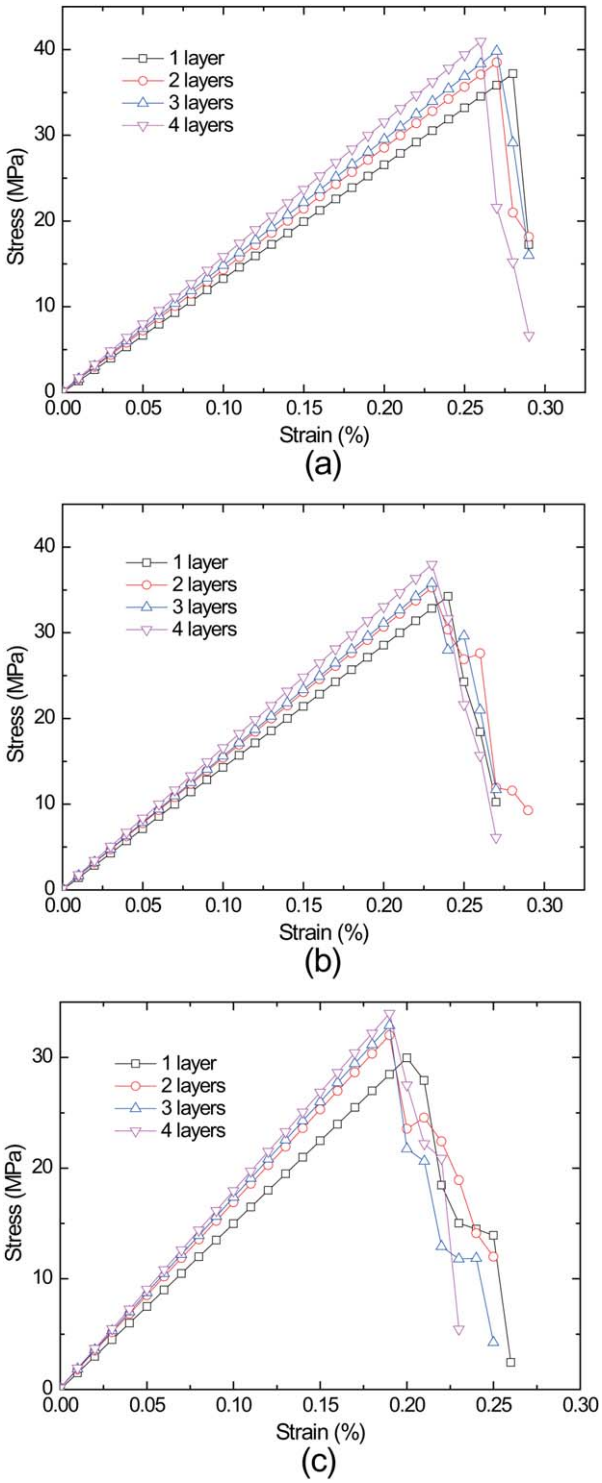

Figure 7. Stress–strain relationships when the nanoparticle Young's moduli are 5, 10, and 100 GPa, respectively. [Color figure can be viewed in the online issue, which is available at wileyonlinelibrary.com.]

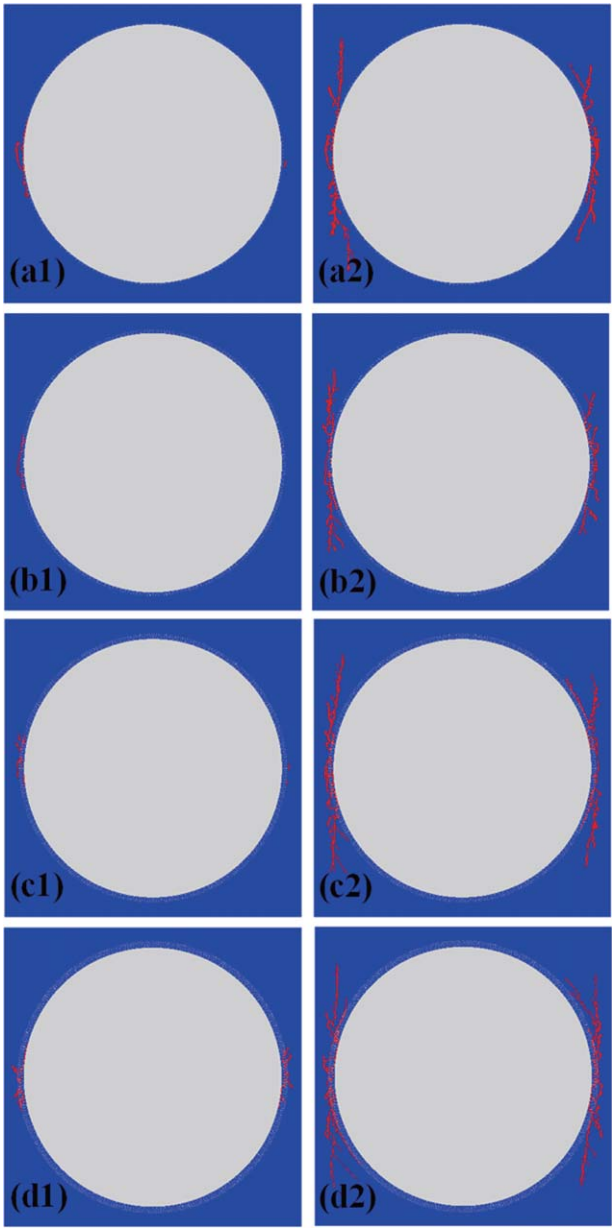

Figure 8. The damage onset and crack propagation within the unit cells with different numbers of nanoparticle layer (red area is the damage onset and crack propagation zone). [Color figure can be viewed in the online issue, which is available at wileyonlinelibrary.com.]

approach, the matrix is assumed to be isotropic material and the maximum principal stress theory is applicable for damage onset prediction.[2,29] To simulate the damage process of matrix, the stress state at each integration point needs to be always monitored. Then by comparing the current stress state with a specific failure criterion (such as maximum principal stress), the material properties are reduced at each "failed" integration point. If the stress level satisfies the failure criterion, the matrix would crack. When failure is detected the degradation is applied only on the elastic modulus by multiplying them with a degradation factor*D*. The matrix was modeled as isotropic with the following stiffness matrix:

$$[C]=[S]^{-1}=\begin{bmatrix} \frac{1}{E\cdot D} & -\frac{v}{E\cdot D} & 0 \\ -\frac{v}{E\cdot D} & \frac{1}{E\cdot D} & 0 \\ 0 & 0 & \frac{1}{G\cdot D} \end{bmatrix}^{-1} \quad (3)$$

The Young's modulus E and the shear modulus G are degraded independently by degradation factor D which initially set equal to unity. During the analysis process, if the stress level exceeds the strength allowed for matrix according to the failure criterion, the modulus are degraded. Here, a degradation factor $D=0$ cannot be used. It may lead to the infinity if it is applied to the terms of the stiffness matrix. The mechanical behavior of the matrix was assumed to be linear elastic until damage was detected. After damage occurred, the response was also linear elastic but with a degraded modulus.

RESULTS AND DISCUSSION

Investigation of the Models Contain One Layer of Nanoparticle

In this subsection, the composite macroscopic stress–strain relationships is studied under uniaxial tensile loading based on the unit cell models with only one layer nanoparticles. Figure 5 shows the simulation results of stress-strain relationships for different nanoparticle-fiber space distances under the same nanoparticle number. The nanoparticle number is 50, 100, and 200 for Figure 5(a–c), respectively. From Figure 5, one can see that whether the nanoparticle-fiber space distance is 40, 100, or 200 nm, the influence of distance between nanoparticle and fiber play little role in the stress–strain relationships under the same nanoparticle number. Although it is an obvious conclusion according to the rule of mixture for composites, in a sense, this conclusion proves that the modeling strategy employed in this study is efficient. However, the nanoparticle number in the micromechanical models does play a significant role in the maximum strengths, corresponding failure strain and effective modulus of composites as shown in Figure 6. Figure 6 shows the simulation results of stress–strain relationships for different nanoparticle numbers under the same nanoparticle-fiber space distance. The nanoparticle-fiber space distance is 40, 100, or 200 nm for Figure 6(a–c), respectively. The nanoparticle number is 50, 100, and 200 for each Figure. Under a transverse tensile loading, numerical results have shown that the ultimate strength in the unit cell model with less nanoparticle is greater than the ultimate strength in the unit cell model with more nanoparticle. For the incorporation of only one layer of nanoparticle, composites failure mode will be simple. At this point, more nanoparticle will produce more interface within the matrix, and damage crack initiation usually starts in the interface. However, it can be found that the more the nanoparticle is, the larger the effective modulus of composites is. These results agree well with the results of Maligno and Warrior.[29] By adding more of the reinforcement, it displays a beneficial effect in terms of the elastic properties.

Investigation of the Models Contain Multilayer Nanoparticles

The composite macroscopic stress–strain relationships are plotted in Figure 7 for different nanoparticle Young's moduli under

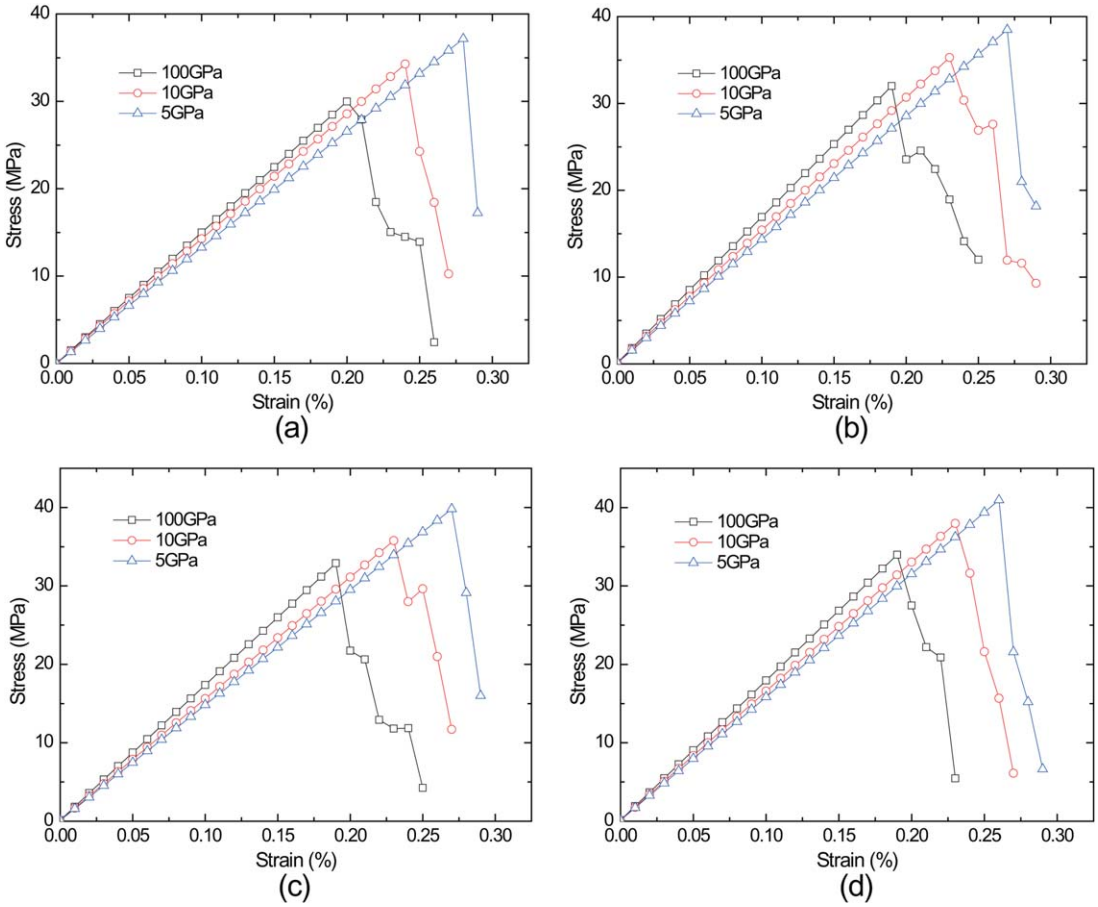

Figure 9. Stress–strain relationships when the number of nanoparticle layer is fixed as one, two, three, and four, respectively. [Color figure can be viewed in the online issue, which is available at wileyonlinelibrary.com.]

uniaxial tensile loading. The nanoparticle Young's moduli are 5, 10, and 100 GPa for Figure 7(a–c), respectively. For each Young's modulus, unit cells with one layer, two layers, three layers, and four layers of nanoparticle are studied. From Figure 7(a–c), one can see that the effective modulus of unit cell which contains more nanoparticals is greater than the effective modulus of unit cell which contains less nanoparticals, which is similar to the results obtained in Investigation of the Models Contain One Layer of Nanoparticle section. Furthermore, it can be found that the ultimate strength of composites is increasing as the number of nanoparticle layer increases. The results demonstrate that multilayer of nanoparticle may induce the bifurcation of the propagating cracks which consumes substantial deformation energy and contributes to the increased failure strain and strength of the composites.[30] Figure 8 displays the damage onset and the following crack propagation within the unit cells with different numbers of nanoparticle layer. The number of nanoparticle layer is one, two, three and four for Figure 8(a–d), respectively. And the nanoparticle Young's modulus is 5 GPa for all the simulations. It can be found that as the number of nanoparticle layer increases the local crack situation tends to increase in complexity.

Effects of the Young's Modulus of Nanoparticle

When the number of nanoparticle layer is fixed as one, two, three and four, the composite macroscopic stress–strain relationships are given in Figure 9 for different nanoparticle Young's modulus, respectively. Nanoparticle with Young's modulus 5, 10, and 100 GPa are studied for each case. Figure 9 shows that the ultimate strength in unit cells with smaller nanoparticle Young's modulus is greater than the ultimate strength in unit cells with larger nanoparticle Young's modulus. It is because stress concentration is easy to occur in the composites with a larger nanoparticle Young's modulus under the same strain loading. However, it can be found that the larger the nanoparticle Young's modulus is, the larger the effective modulus of composites is. These results are similar with the results in Figure 6 and agree with the results of Maligno and Wang.[29,31] Both nanoparticle number and nanoparticle Young's modulus play a significant role in the mechanical properties of the interphase.

CONCLUSIONS

A new method and a micromechanical model are developed for the mechanical property prediction of fiber- and nanoparticle-reinforced composites. Based on the models, a series of micromechanical computational experiments lead us to following conclusions:

a. The distance between nanoparticle and fiber play little role in the stress-strain relationship under the same nanoparticle number.

b. Both the ultimate strength and the effective modulus of composites increase as the increase of the number of nanoparticle or nanoparticle layer.
c. The ultimate strength of composites increases as the decrease of the nanoparticle Young's modulus; the effective modulus of composites is just the opposite.
d. The results demonstrate that the bifurcation of the propagating cracks can increase the strength of the composites, and complex crack situation can be introduced by the increase of the number of nanoparticle layer.

ACKNOWLEDGMENTS

This work was financially supported by the Scientific Research Fund of Liaoning Provincial Education Department (L2013078) and the Doctoral Start-up Foundation of Shenyang Aerospace University (13YB13). The financial contributions are gratefully acknowledged.

REFERENCES

1. Daniel, I. M.; Ishai, O. Engineering Mechanics of Composite Materials; New York: Oxford University Press, **1994**.
2. Melro, A. R.; Camanho, P. P.; Pinho, S. T. *Compos. Sci. Technol.* **2008**, *68*, 2092.
3. Zohdi, T. I.; Wriggers, P. An Introduction to Computational Micromechanics; Springer: Germany, **2008**.
4. Shan, Z.; Gokhale, A. M. *Comput. Mater. Sci.* **2002**, *24*, 361.
5. Aghdam, M. M.; Falahatgar, S. R. *Compos. Struct.* **2004**, *66*, 415.
6. Matzenmiller, A.; Gerlach, S. *Compos. B Eng.* **2005**, *37*, 117.
7. Qing, H. *Mater. Des.* **2013**, *51*, 438.
8. Shokrieh, M. M.; Nasir, V.; Karimipour, H. *Mater. Des.* **2012**, *35*, 394.
9. Yu, M.; Zhu, P.; Ma, Y. *Mater. Des.* **2013**, *47*, 80.
10. Wang, Z.; Wang, X.; Zhang, J.; Liang, W.; Zhou, L. *Mater. Des.* **2011**, *32*, 885.
11. Sozhamannan, G. G.; Prabu, S. B.; Paskaramoorthy, R. *Mater. Des.* **2010**, *31*, 3785.
12. Davis, D. A.; Wilkerson, J. W.; Zhu, J.; Ayewah, D. A. A. *Compos. Struct.* **2010**, *92*, 2653.
13. Wetzel, B.; Haupert, F.; Zhang, M. Q. *Compos. Sci. Technol.* **2003**, *63*, 2055.
14. Gojni, F. H.; Wiechmann, M. H. G.; Köppke, U.; Fiedler, B.; Schulte, K. *Compos. Sci. Technol.* **2004**, *64*, 2363.
15. Schadler, L. S.; Ajayan, P. M.; Schadler, L. S.; Braun, P. V. *Nanocompos. Sci. Technol.* **2003**, 77.
16. Tjong, S. C. *Adv. Eng. Mater.* **2007**, *9*, 639.
17. Vassileva, E.; Friedrich, K. *J. Appl. Polym. Sci.* **2003**, *89*, 3774.
18. Pöllänen, M.; Pelz, U.; Suvanto, M.; Pakkanen, T. T. *J. Appl. Polym. Sci.* **2010**, *116*, 1218.
19. Bhattacharyya, A.; Rana, S.; Parveen, S.; Fangueiro, R.; Alagirusamy, R.; Joshi, M. *J. Appl. Polym. Sci.* **2013**, *129*, 2383.
20. Liu, L.; Li, L.; Gao, Y.; Tang, L.; Zhang, Z. *Compos. Sci. Technol.* **2013**, *77*, 101.
21. Hua, Y.; Gu, L.; Watanabe, H. *Int. J. Eng. Sci.* **2013**, *69*, 69.
22. Zhang, B.; Yang, Z.; Sun, X.; Tang, Z. *Comput. Mater. Sci.* **2010**, *49*, 645.
23. Yang, L.; Yan, Y.; Liu, Y.; Ran, Z. *Compos. Sci. Technol.* **2012**, *72*, 1818.
24. Wacker, G.; Bledzki, A. K.; Chate, A. *Compos. A* **1998**, *29*, 619.
25. Comte, C.; von Stebut, J. *Surf. Coat. Technol.* **2002**, *154*, 42.
26. Jang, J.-S.; Kim, H.-i.; Gibson, R. F.; Suhr, J. *Mater. Des.* **2013**, *51*, 219.
27. Altenbach, H.; Tushtev, K. *Mech. Compos. Mater.* **2001**, *37*, 5.
28. Blackketter, D.; Walrath, D. E.; Hansen, A. C. *J. Compos. Tech. Res.* **1993**, *15*, 136.
29. Maligno, A. R.; Warrior, N. A.; Long, A. C. *Compos. Sci. Technol.* **2010**, *70*, 36.
30. Jiang, Z.; Zhang, H.; Zhang, Z.; Murayama, H.; Keiji, O. *Compos. A* **2008**, *39*, 1762.
31. Wang, X.; Zhang, J.; Wang, Z.; Zhou, S.; Xinyang, S. *Mater. Des.* **2011**, *32*, 3486.